

Influence of Boriding Process in Adhesion of CVD Diamond Films on Tungsten Carbide Substrates

Raonei Alves Campos^{a,*}, Andre Contin^b, Vladimir Jesus Trava-Airoldi^b, Danilo Maciel Barquete^c,
João Roberto Moro^a, Evaldo José Corat^b

^aInstituto Federal de Educação, Ciência e Tecnologia de São Paulo – IFSP, Rua Antônio Fogaça de Almeida, s/n, Jardim Elza Maria, CEP 12322-030, Jacareí, SP, Brazil

^bInstituto Nacional de Pesquisas Espaciais – INPE, Av. dos Astronautas, 1758, Jardim da Granja, CEP 12227-010, São José dos Campos, SP, Brazil

^cUniversidade Estadual de Santa Cruz – UESC, Campus Soane Nazaré de Andrade, Rodovia Jorge Amado, Km 16, Salobrinho, CEP 45662-900, Ilhéus, BA, Brazil

Received: September 22, 2014; Revised: August 31, 2015

This paper shows successful hindering of the negative effects of the cobalt binder in the process of coating WC-Co cutting tools with CVD diamond films. The strategy was creating a boron-rich layer on the surface of the WC-Co substrates as an interlayer to block Co migration. The traditional boriding technique was improved by preheating the salt powders and controlling the brittle region thickness in the substrate surface. These procedures produce a tougher surface for diamond growth. Adding CF₄ to the gas mixture also enhanced diamond adhesion to the surface. The adhesion of diamond films to WC-Co substrates was evaluated by indentation tests. Samples were characterized by Scanning Electron Microscopy (SEM), Energy Dispersive X-ray (EDX), X-ray Diffraction (XRD) and Raman Scattering Spectroscopy (RSS).

Keywords: boriding, HFCVD, diamond film, diffusion

1. Introduction

Sintered tungsten carbide (WC-Co) manufactured by powder metallurgy is widely used to produce cutting tools for the machining industry. CVD diamond coating is a great alternative to increase cutting tools lifetime for machining nonferrous metals. However, there are still fundamental technological issues to overcome concerning adhesion of the coating to substrate surface. The cobalt (Co) presence in WC-Co is of fundamental importance for the final mechanical properties of the tool, namely toughness, compressive strength and transverse rupture strength, which are fundamental requirements for cutting tools applications. However, cobalt chemically interacts with carbon atoms during chemical vapor deposition of diamond films due to its 3d incomplete sublevel, producing a graphitic phase¹⁻³ on the substrate surface, inhibiting the direct deposition of CVD diamond films on WC-Co. Several pretreatments to avoid Co harmful effects have been tried, as shown in literature⁴⁻⁶. Boriding technique⁷ forms an intermediate barrier that blocks Co diffusion to the substrate surface, minimizing the Co binder negative effects for diamond growth. Boriding is one of the pretreatments used in this work. It consists on boron thermomodification from heated powders mixed according to pre-established mass proportions.

As previously published⁸ the addition of CF₄ in the gas phase promotes the formation of solid carbons, including diamond. Halogens, as atomic hydrogen, chemically react

with graphitic phases, preferentially to react with diamond. The CF₄ addition in the gas phase promotes selective etching of W from WC-Co matrix, forming a C rich surface, from where diamond nucleation starts. This “in situ” WC etching enhance diamond film adhesion. Previous studies suggest that the CF₄ is effective to etch the cobalt binder phase from the WC-Co surface⁹.

In this paper, we show clearly that brittleness is due to cobalt diffusion out of the substrate during the heating stage of boriding salt to process temperature. Additionally, our diamond growth experiments take advantage of the already known CF₄ beneficial effects for growth on WC-Co substrates.

2. Experimental

ISO K10 WC-Co samples of WC grain size of 0.8µm and containing 6 wt% of Co were used as substrate material. A low speed diamond saw (South Bay Technology model 650) was used to cut commercial drills and bars into disk-shape, 10mm diameter and 2mm thick samples. Each sample was polished with diamond paste 6µm and 1µm grit sizes. The boriding process used powders mixture of boron carbide (B₄C - 15%), silicon carbide (SiC - 70%), potassium fluoroborate (KBF₄ - 10%) and graphite (C - 5%). Boron carbide (B₄C) is the main boron source to form the boron-rich interlayer. SiC in excess during the thermomodification process avoids boron oxide formation. KBF₄ acts as a catalyst to

*e-mail: raoneialves@gmail.com

reduce salt bath melting temperature. Graphite powder it added to balance the reaction.

The boriding process was carefully controlled in all of the stages. Even though CoW_2B_2 and CoWB stable Co phases work as an efficient barrier to Co diffusion, they also embrittles the substrate surface, mainly when using fine grain WC-Co substrates. In order to control surface brittleness, by controlling the thickness of those commonly formed brittle regions, we modified the traditional boriding process. Initially, we heated the powder mixture, in a stainless steel crucible, up to $1000\text{ }^\circ\text{C}$ and kept at this temperature for 15 min. The sample was then placed into the crucible for the thermodiffusion process, with temperature kept constant at $1000\text{ }^\circ\text{C}$, for 5h. After this, the sample was removed at high temperature, with salt mixture still melted, to simplify handlings and excess powders cleaning. Sample preparation was completed with chemical etching¹⁰, according to Table 1.

Chemical etching starts with Caro's acid followed by Murakami's alkaline etching. The acid etching removes cobalt residues^{11,12} from the surface after heat treatment. The Murakami's solution specifically etches WC grains^{13,14} to increase surface roughness.

Previous to the CVD diamond growth, the samples were pre-treated in an ultrasonic bath with a $0.25\mu\text{m}$ diamond powder suspension in n-hexane for 1h to increase diamond nucleation rate¹⁵. Diamond growth was performed in a hot filament reactor with six straight tungsten filaments, $125\mu\text{m}$ diameter. Filament temperature was kept at $2200\text{ }^\circ\text{C}$. All films were deposited for 5h in a gaseous atmosphere of methane (2%), carbon tetrafluoride CF_4 (2%) and hydrogen (96%). The total flow-rate was 100sscm and reactor pressure was $6.5 \times 10^3\text{ Pa}$ ¹⁶.

A tungsten resistance placed in the substrate holder was used to control substrates temperature at chosen level, in

Table 1. Chemical etching parameters used in WC-Co.

Solution	Parameters	Time
Murakami's	$\text{KOH} + \text{K}_3[\text{Fe}(\text{CN})_6] + \text{H}_2\text{O} - 1:1:10$	10min
Caro's acid	$\text{H}_2\text{SO}_4 + \text{H}_2\text{O}_2 - 1:5$	15s

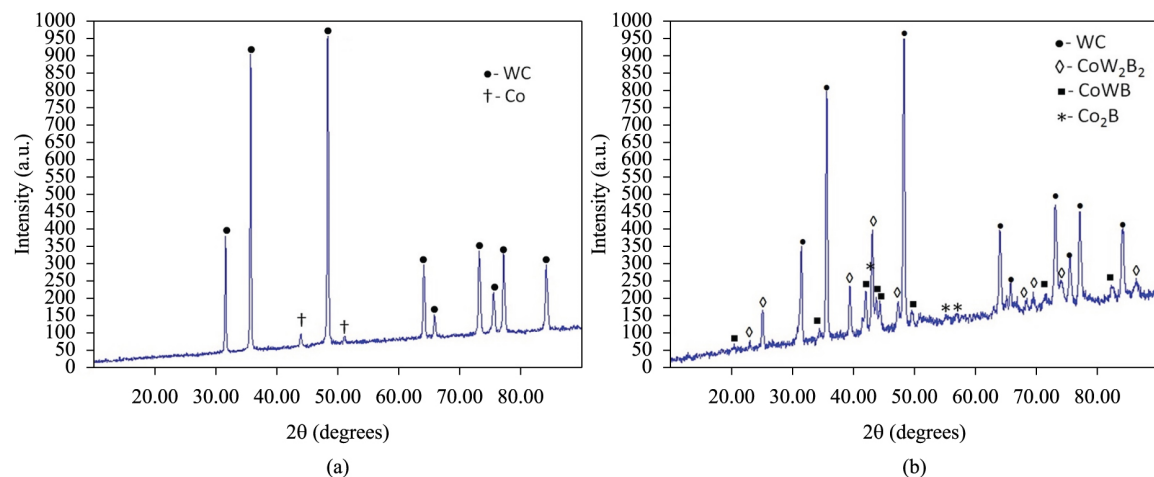


Figure 1. (a) X-ray diffractograms of the WC-Co sample prior to the boriding process, (b) after controlled boriding process.

the range of $700\text{ }^\circ\text{C}$ to $900\text{ }^\circ\text{C}$. Adhesion tests of diamond films were performed in a Rockwell C indenter¹⁷⁻¹⁹. Applied loads ranged from 300 N to 700 N. Gradual variation of loads allowed measurement of critical loads supported by each diamond film²⁰.

Samples were characterized by Scanning Electron Microscopy (SEM), Energy Dispersive X-ray (EDX), X-ray Diffraction (XRD) and Raman Scattering Spectroscopy (RSS). Residual stresses in diamond films were evaluated considering the deviation from the Raman shift of stress-free diamond, of 1332 cm^{-1} . Raman spectroscopy was performed with Renishaw System 2000, using argon laser excitation (514.5 nm). Microscopic evaluation of surface morphology and interface were performed with Jeol (JSM-5310) Scanning Electron Microscope (SEM). An energy dispersive X-ray detector attached to the SEM enabled evaluation of the elemental distribution in the interface (EDS). A Philips X'Pert MRD X-ray Diffractometer was used to evaluate phases in the substrate surface before and after boriding.

3. Results and Discussion

Figures 1a and 1b show X-ray diffractograms of the WC-Co sample, prior and after the boriding process, respectively. As it can be noticed on Figure 1a, only WC and Co are present in the substrate before boriding, while other phase as CoW_2B_2 , CoWB and Co_2B form after boriding treatment. Small fractions of Co_2B were formed due to free Co binder that migrated to surface from bulk WC-Co.

Our early experiments^{2,21}, as other previous reports²², showed that a brittle region formed in the substrate surface during salt powders heating stage to the boriding process temperature. Edwards et al.²¹ used WC-TiC-Co samples with medium grain size of nearly $3\mu\text{m}$ and did not report this brittle region. However, this brittle region always formed in our experiments with $0.8\mu\text{m}$ grain size WC-Co substrates²³.

Figure 2 shows this brittle region after traditional boriding. A WC skeleton without any binder is shown in the figure, in the region indicated as "a". A boride interlayer formed under this skeleton, indicated as region "b" in the figure. This brittle skeleton, clearly seen in Figure 2, is

formed due to cobalt migration to the surface of the sample during the heating stage, before reaching the boriding process temperature. The sample shown in Figure 2 has a large brittle region. However, for samples with small WC grain, as those used in this work, even a very thin brittle interface is unfavorable for tool applications, resulting in fragile coating. Indentation tests confirmed the weakness of the resulting coating - diamond films/boride interlayer as shown in the Figure 3, where the delamination of the 6 μ m thick diamond film around indentation mark can be seen. This round broad delamination is typical for low adherent films. As previously stated, the low adherence is due to the brittle interface formed in the region with a WC skeleton.

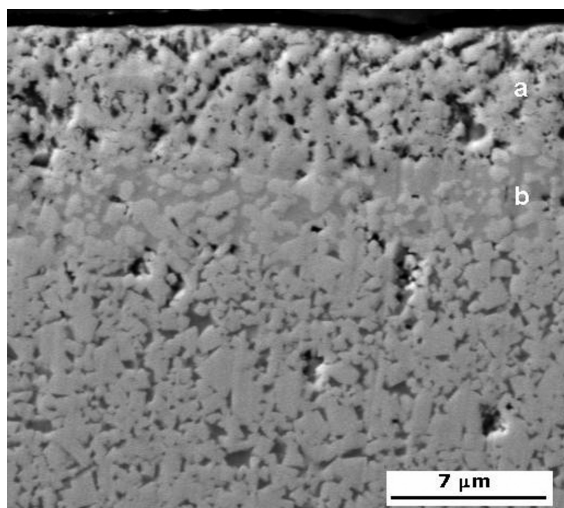


Figure 2. SEM image of the cross section of WC-Co substrate after traditional boriding process. Detail (a) shows the brittle region and (b) the boride interlayer that blocks Co diffusion to surface.

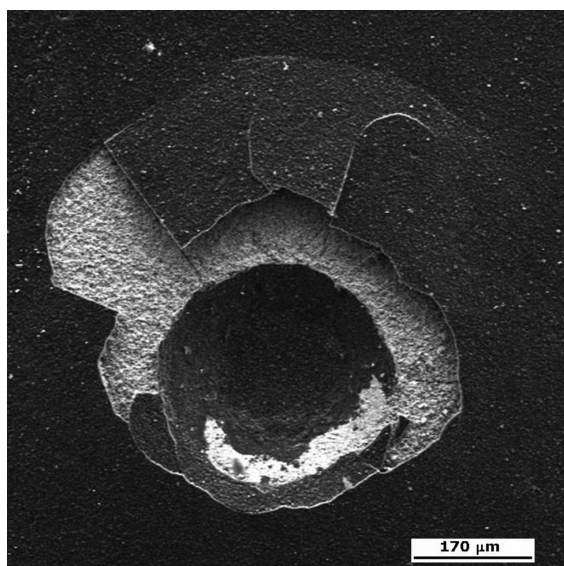


Figure 3. SEM image of the diamond film deposited on WC-Co substrate with boride interlayer, loaded at 600N using a Rockwell C indenter.

The stable CoW_2B_2 and CoWB cobalt compounds were not formed in this region, probably due to Co thermal migration to substrate surface.

Figure 4 shows the result of our controlled boriding method. Insertion of samples after preheating powders prevented the formation of a brittle region in the boride interlayer. The boride interface starts at the surface without any brittle region. Preheating the powders doesn't affect CoW_2B_2 and CoWB phases formation. These are the main phases responsible for the boriding barrier. Further, they minimize the presence of unreacted Co on surface.

Even with small amounts of free Co in surface, we further improved the interface by chemical etching. Caro's solution removed cobalt residues and Murakami's solution reacts with WC to get a rougher surface. Figure 5a shows the surface morphology after chemical attack with Caro's and Murakami's reagents. Figure 5b shows a SEM image of diamond film deposited on WC-Co substrate with a boride interlayer. The deposited diamond films had an average thickness of 6 μ m for the typical 5h growth period.

The diamond film adhesion on the WC-Co substrate significantly increased with the controlled boring process. Figure 6 shows indentation imprints on these samples. No lateral cracks formed at loads up to 700N using the Rockwell C indenter. Figures 6a shows the imprint for 300N load, with a slight crack formed on the CVD diamond film on the sample. Figure 6b shows de imprint for 500N. The diamond film breaks up concentrically around the indentation mark due to boriding interlayer and substrate deformation with load increasing and without peeling off the diamond film. Even at loads of 600N and 700N (Figures 6c and 6d), the diamond films showed similar mechanical behaviors to the one shown in Figure 6b. At critical load of 700N, the diamond film collapsed, as shown in Figure 6d. The good diamond film adhesion demonstrated on Figure 6 suggests that brittle regions on the substrate surface were not formed in the boriding process.

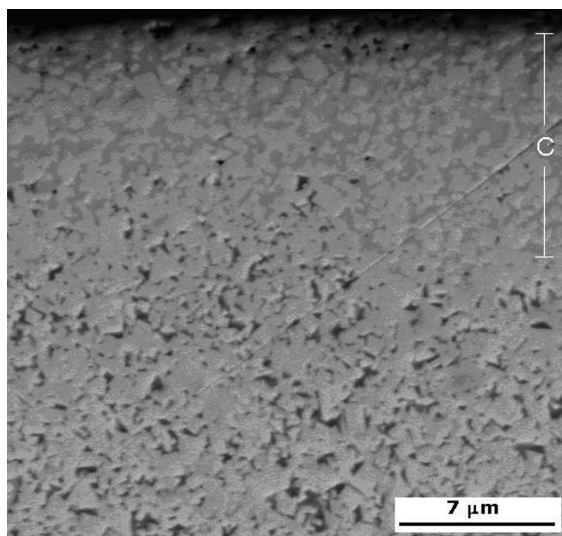


Figure 4. SEM image of the cross section of WC-Co substrate after controlled boriding, with samples immersed on powders after heating up to process temperature. Detail (c) shows the boride interlayer without the brittle region.

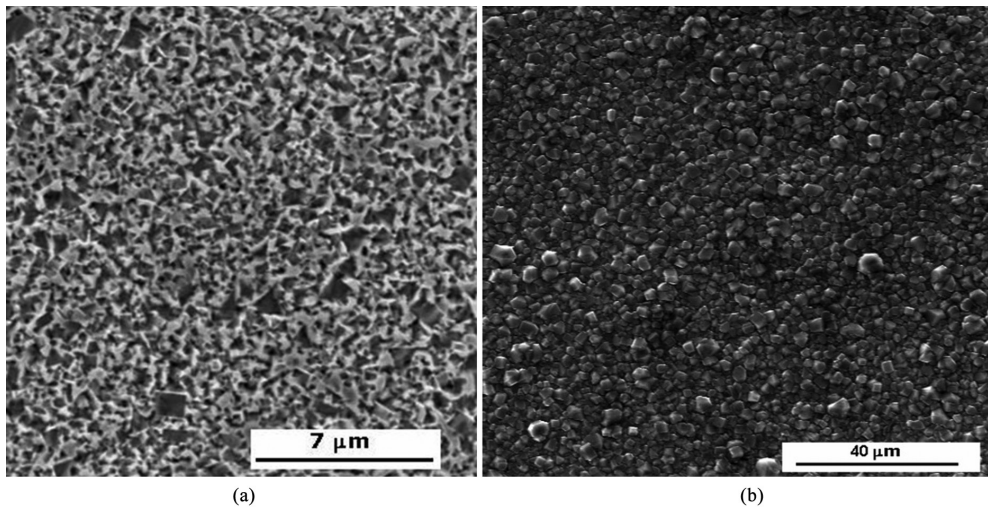


Figure 5. (a) SEM image of the substrate surface etched and (b) diamond film deposited on the WC-Co with the controlled boriding layer.

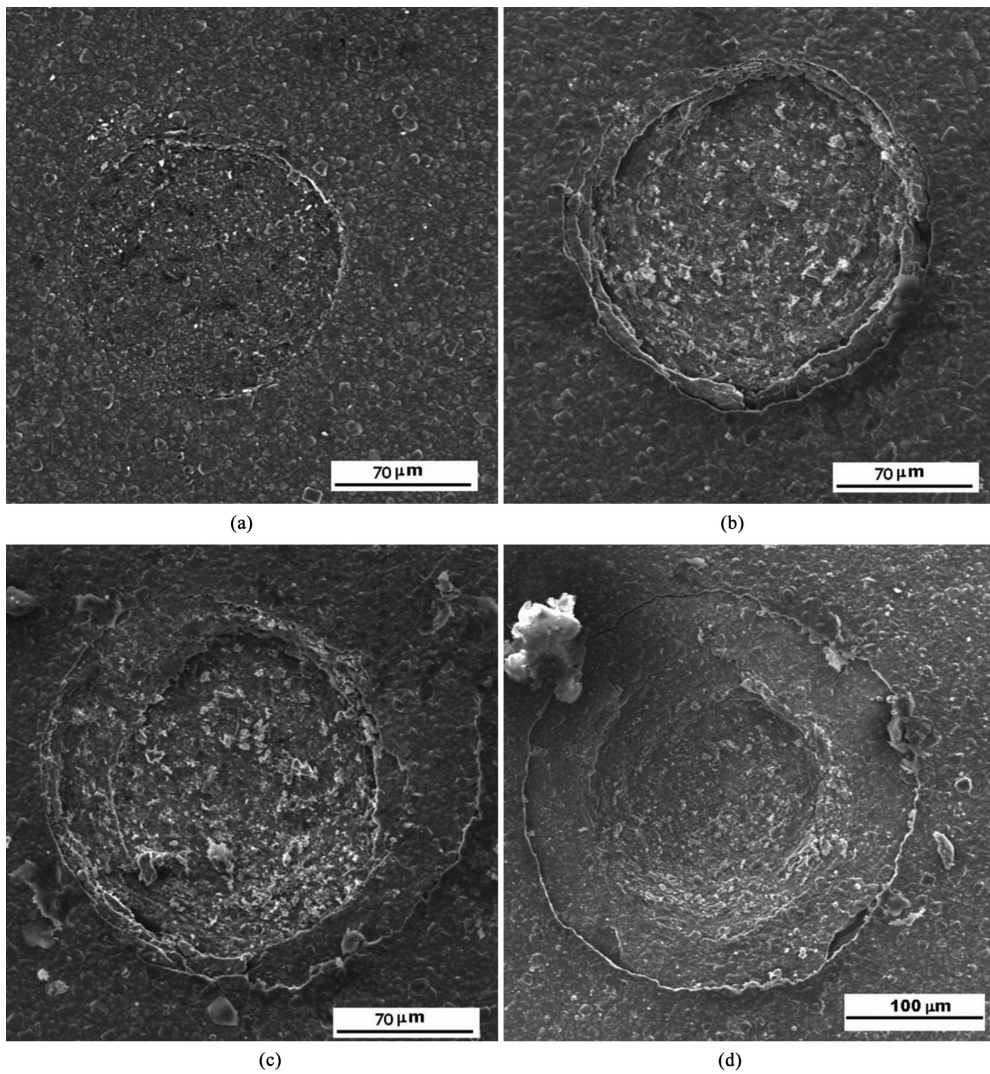


Figure 6. SEM image of indentation imprints at different indentation loads– 300N (a), 500N (b), 600N(c) and 700N (d).

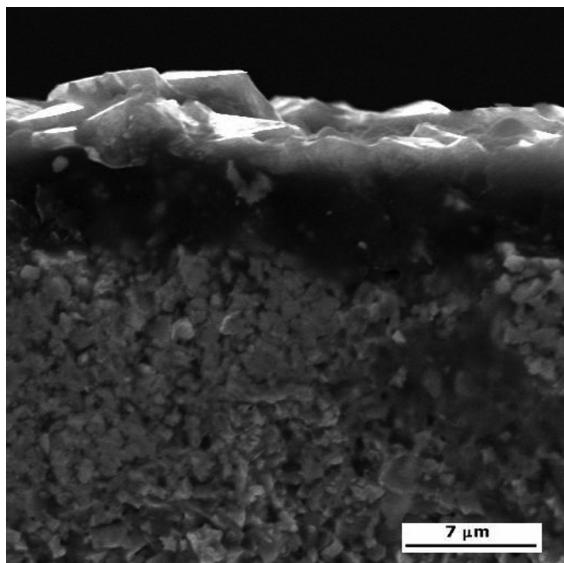


Figure 7. SEM image of a cross section of the diamond film deposited on the WC-Co with controlled boride interlayer. This cross section corresponds to the fracture surface of the sample during indentation test.

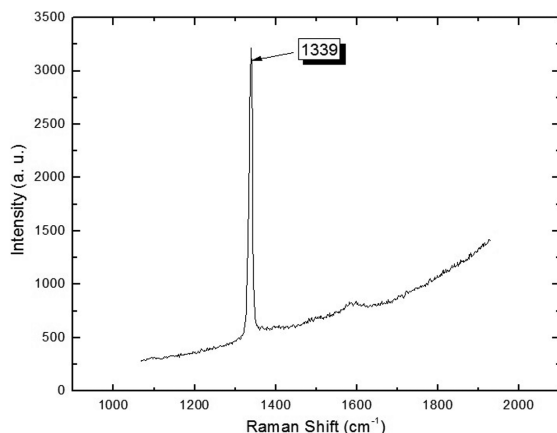


Figure 8. Raman spectrum of diamond film on WC-Co with controlled boride interlayer.

References

- Chandran M, Kumaran CR, Gowthama S, Shanmugam P, Natarajan R, Bhattacharya SS, et al. Chemical vapor deposition of diamond coatings on tungsten carbide (WC-Co) riveting inserts. *Journal of Refractory Metals and Hard Materials*. 2013; 37:117-120. <http://dx.doi.org/10.1016/j.jrmhm.2012.11.005>.
- Campos RA, Contin A, Trava-Airoldi VJ, Barquete DM, Corat EJ, Canale L, et al. CVD of alternated MCD and NCD films on cemented carbide inserts. *Journal of ASTM International*. 2011; 8(3):103242. <http://dx.doi.org/10.1520/JAI103242>.
- Yang T, Wei Q, Qi Y and Yu Z. The diffusion behavior of carbon in sputtered tungsten film and sintered tungsten block and its effect on diamond nucleation and growth. *Diamond and Related Materials*. 2015; 52:49-58. <http://dx.doi.org/10.1016/j.diamond.2014.12.009>.

During Rockwell C indentation tests, at 600N load, due to flaws on substrate base, a sample broke into two pieces without peeling off, as shown in Figure 7. This is a relevant fact that can be correlated to good adhesion of the diamond film to the substrate surface. This also indicates high interface adhesion for all interfaces - substrate to boride interlayer and boride to diamond film.

Figure 8 shows the Raman spectrum for the diamond film deposited on WC-Co substrate with boride interlayer. Residual stresses in diamond films, typically compressive due to the smaller thermal expansion coefficient of diamond in comparison to WC-Co substrate^{24,25}, can be evaluated from Raman peak displacement relative to natural unstressed diamond^{26,27}. In this case, the peak is near to 1339 cm^{-1} , corresponding to a displacement of 7.1 cm^{-1} from the natural diamond peak at 1332 cm^{-1} wavenumber. This leads to calculated compressive stress of 4.0GPa in the deposited diamond film.

4. Conclusion

In this work we have shown that the initial stage of the boriding process is critical to get strong interfaces to sub-micrometric grain size WC-Co substrates. In this stage Co migrates out the WC-Co as the boriding bath is heated up, producing a fragile surface. Inserting the sample at the final boriding temperature, when the bath is already melted and stable, minimizes this brittleness effect and the brittle region disappears. The acid etching after boriding cleans the surface from residual free cobalt. The combined etching effects of the alkaline Murakami solution and the “in situ” CF_4 gas are effective to increase WC surface roughness to improve diamond nucleation. The surface roughness of the substrate also enables formation of better interlocking and hence higher adhesion strength. The association of these good conditions with a tough boride interlayer enabled the deposition of good quality and adherent diamond films on WC-Co substrates, as shown by Raman spectroscopy and indentation tests.

Acknowledgements

The authors would like to acknowledge IFPR (Instituto Federal de Educação, Ciência e Tecnologia do Paraná) and INPE for financial support of this work.

- Hojman E, Akhvlediani R, Layous A and Hoffman A. Diamond CVD film formation onto WC-Co substrates using a thermally nitrated Cr diffusion-barrier. *Diamond and Related Materials*. 2013; 39:65-72. <http://dx.doi.org/10.1016/j.diamond.2013.08.002>.
- Ali N, Cabral G, Lopes AB and Gracio J. Time-modulated CVD on 0.8 μm -WC-10%-Co hard metals: study on diamond nucleation and coating adhesion. *Diamond and Related Materials*. 2004; 13(3):495-502. <http://dx.doi.org/10.1016/j.diamond.2003.12.001>.
- Vandierendonck K, Nesládek M, Kaldec S, Quaeysaegens C, Stappen MV and Stals LMM. W/WC diffusion barrier layers for CVD diamond coatings deposited on WC-Co: microstructure and properties. *Surface and Coatings Technology*. 1998; 98(1-3):1060-1065. [http://dx.doi.org/10.1016/S0257-8972\(97\)00553-7](http://dx.doi.org/10.1016/S0257-8972(97)00553-7).

7. Wang Q, Zhang Q, Wang SG, Yoon SF and Ahn J, Zhao B, et al. Effects of pretreatment on the performance of diamond coated cemented carbide cutting tools. *Journal of Vacuum Science & Technology A*. 2003; 21(6):1939-1942. <http://dx.doi.org/10.1116/1.1619419>.
8. Barquete DM, Resende LW, Corat EJ, Trava-Airoldi VJ and Neto CM. *Diamond chemical vapor deposition on cutting tools*. SAE International; 1998. p. 1-7. SAE Technical Paper Series.
9. Almeida FA, Soares E, Fernandes AJS, Sacramento J, Silva RF and Oliveira FJ. Diamond film adhesion onto sub-micrometric WC-Co substrates. *Vacuum*. 2011; 85(12):1135-1139. <http://dx.doi.org/10.1016/j.vacuum.2010.12.025>.
10. Kamiya S, Takahashi H, Polini R and Traversa E. Quantitative determination of the adhesive fracture toughness of CVD diamond to WC-Co cemented carbide. *Diamond and Related Materials*. 2000; 9(2):191-194. [http://dx.doi.org/10.1016/S0925-9635\(00\)00229-6](http://dx.doi.org/10.1016/S0925-9635(00)00229-6).
11. Polini R and Barletta M. On the use of CrN/Cr and CrN interlayers in hot filament chemical vapour deposition (HF-CVD) of diamond films onto WC-Co substrates. *Diamond and Related Materials*. 2008; 17(3):325-335. <http://dx.doi.org/10.1016/j.diamond.2007.12.059>.
12. Meng XM, Tang WZ, Hei LF, Li CM, Askari SJ and Chen GC. Application of CVD nanocrystalline diamond films to cemented carbide drills. *International Journal of Refractory Metals & Hard Materials*. 2008; 26(5):485-490. <http://dx.doi.org/10.1016/j.ijrmhm.2007.11.006>.
13. Haubner R, Kubelka S, Lux B, Griesser M and Grasserbauer M. Murakami and H₂SO₄/H₂O₂ pretreatment of WC-Co hard metal substrates to increase the adhesion of CVD diamond coatings. *Journal de Physique - IV France*. 1995; 5:753-760.
14. Sarangi SK, Chattopadhyay A and Chattopadhyay AK. Influence of process parameters on growth of diamond crystal on cemented carbide substrates by HFCVD system. *International Journal of Refractory Metals & Hard Materials*. 2012; 31:1-13. <http://dx.doi.org/10.1016/j.ijrmhm.2011.07.007>.
15. Souza TM, Trava-Airoldi VJ, Corat EJ and Leite NF. Pretreatment and pos-treatment for enhanced adherence of the diamond-CVD films on Ti₆Al₄V substrate using hot filament assisted technique. *Revista Brasileira de Vacuo*. 1997; 16:22-25.
16. Silva VA, Corat EJ and Silva CRM. Influence of CF₄ addition for HFCVD diamond growth on silicon nitride substrates. *Diamond and Related Materials*. 2001; 10(11):2002-2009. [http://dx.doi.org/10.1016/S0925-9635\(01\)00468-X](http://dx.doi.org/10.1016/S0925-9635(01)00468-X).
17. Wei Q, Yu ZM, Ashfold MNR, Ma L and Chen Z. Fretting wear and electrochemical corrosion of well-adhered CVD diamond films deposited on steel substrates with a WC-Co interlayer. *Diamond and Related Materials*. 2010; 19(10):1144-1152. <http://dx.doi.org/10.1016/j.diamond.2010.04.004>.
18. Lai WC, Wu Y, Chang H and Lee Y. Enhancing the adhesion of diamond films on cobalt cemented tungsten carbide substrate using tungsten particles via MPCVD system. *Journal of Alloys and Compounds*. 2011; 12(12):4433-4438. <http://dx.doi.org/10.1016/j.jallcom.2011.01.149>.
19. Zhang JG, Wang XC, Shen B and Sun FH. Effect of boron and silicon doping on improving the cutting performance of CVD diamond coated cutting tools in machining CFRP. *International Journal of Refractory Metals & Hard Materials*. 2013; 41:285-292. <http://dx.doi.org/10.1016/j.ijrmhm.2013.04.017>.
20. Campos RA, Contin A, Trava-Airoldi VJ, Moro JR, Barquete DM and Corat EJ. CVD diamond films growth on silicon nitride inserts (Si₃N₄) with high nucleation density by functionalization seeding. *Materials Science Forum*. 2012; 727-728:1433-1438. <http://dx.doi.org/10.4028/www.scientific.net/MSF.727-728.1433>.
21. Edwards E. *Estudos da formação de interface de boreto para a deposição de diamante CVD*. [Thesis]. São José dos Campos: Instituto Nacional de Pesquisas Espaciais; 2008.
22. Lin G, Zhang Z, Qiu Z, Luo X, Wang J and Zhao F. Boronizing mechanism of cemented carbides and their wear resistance. *International Journal of Refractory Metals & Hard Materials*. 2013; 41:351-355. <http://dx.doi.org/10.1016/j.ijrmhm.2013.05.008>.
23. Campos RA. *Estudo da deposição de filmes de diamante CVD sobre carbeto de tungstênio, com interface controlada de boreto*. [Thesis]. São José dos Campos: Instituto Nacional de Pesquisas Espaciais; 2009.
24. Buijnsters JG, Shankar P, Gopalakrishnan P, van Enkevort WJP, Schermer JJ and Ramakrishnan SS. Diffusion modified boride interlayers for chemical vapour deposition of low-residual-stress diamond films on steel substrates. *Thin Solid Films*. 2003; 426(1-2):85-93. [http://dx.doi.org/10.1016/S0040-6090\(03\)00013-0](http://dx.doi.org/10.1016/S0040-6090(03)00013-0).
25. Nibennaoune Z, George D, Ahzi S, Ruch D, Remond Y and Gracio JJ. Numerical simulation of residual stresses in diamond coating on Ti-6Al-4V substrate. *Thin Solid Films*. 2010; 518(12):3260-3266. <http://dx.doi.org/10.1016/j.tsf.2009.12.092>.
26. Ager JW 3rd and Drory MD. Quantitative measurement of residual biaxial stress by Raman spectroscopy in diamond grown on a Ti alloy by chemical vapor deposition. *Physical Review B, Condensed Matter*. 1993; 48(4):2601-2607. <http://dx.doi.org/10.1103/PhysRevB.48.2601>. PMID:10008655.
27. Ali N, Cabral G, Neto VF, Sein H, Ahmed W, and Gracio J. Surface engineering of WC-Co used in dental tools technology. *Materials Science and Technology*. 2003; 19(9):1273-1278. <http://dx.doi.org/10.1179/026708303225005962>.